EasyChair Preprint

№ 10023

Single Scan Track Analysis of Selective Laser Melted AlSi10Mg Alloy

Bonagiri Sai Charan, Mergoju Srikanth, B Pazhanivel and Deepak Kumar Pattanayak

May 9, 2023

Single scan track analysis of selective laser melted AlSi10Mg alloy

B. Sai Charan[1,2,3] , M. Srikanth[1,2,3], B. Pazhanivel[2] and Deepak K. Pattanayak[1,2,3]

[1]Process Engineering Division, CSIR- Central Electrochemical Research Institute, Karaikudi- 630003,Tamil Nadu, India

[2]Additive Manufacturing Facility, CSIR-Central Electrochemical Research Institute, Karaikudi 630003, Tamil Nadu, India

[3]Academy of Scientific and Innovative Research (AcSIR), Ghaziabad- 201002, India

**Corresponding author: Deepak K. Pattanayak, Email: deepak@cecri.res.in, pattanayak1977@gmail.com*

Abstract:

Additive manufacturing (AM) is a booming technology and has been used to fabricate customized and complex design components for various structural applications. The features of aluminium alloys such as low density, high strength-to-weight ratio, great thermal and electrical conductivity, etc. attract to make components usingthe AM technology. Selective laser melting (SLM) one of the AM process has recently gained more popularity over the past several years due to its design flexibility, non-equilibrium microstructure, excellent mechanical characteristics, and high solid solubility etc.However, because of more reflectivity than other metals, SLM of aluminium alloys becomes a challenging process. Many process-related difficulties in the SLM process for aluminium alloy are still poorly understood and needs to be systematically addressed.

Here, the shape and size of the melt pool in the single scan tracks method of SLM process is explored using AlSi10Mg alloy as a candidate material.Process parameters involved in SLM such as laser power and scanning speed are varied during the processing of Aluminium alloy.It was found that laser power and scan speed significantly affects the melt pool geometry. Interestingly, with the increase in laser power from 200 to 370W and the simultaneous decrease in scan speed from 1700 to 300 mm/s, the melt pool width as well as depth increases and vice versa. The results are compared and correlated with the available literatures.

Keywords: Additive manufacturing, selective laser melting, laser power, laser scanning speed, AlSi10Mg.

1. Introduction:

In recent years, additive manufacturing (AM) technologies are getting more attention because of their efficiency, minimal raw material wastage during production, and flexibility to build complex geometries. These technologies are already entered into various fields like automotive, aerospace, energy, structural, defence and biomedical etc. In AM processes, it is important to select the appropriate technology for fabrication of components based on the application and requirement such as porosity, dimensional accuracy, surface roughness, mechanical strength etc. Selective laser melting (SLM) is one of the AM technology based on the laser powder bed fusion technique capable of fabricating complex geometry structures from metal powders. The fabrication of complex geometries mainly depends on the computer-aided design (CAD) model. The CAD models are subsequently converted to .STL format for slicing the design into several layers before sending the design information to the machine. According to the design information, fabrication takes place layer by layer process until the final layer is built up. The fabrication process begins with the layering of powder of predefined thickness uniformly onto the build platformwith the help of a re-coater blade. After powder layering, laser beamselectively scans the area according to the design model using pre-defined processing parameters such as laser power, scan speed, and hatch spacing etc. After the completion of the first layer scanning and melting of metal powder, build platform moves downside for pre-defined layer thickness. Subsequently the re-coaterblade again moves across the base plate for layering the powder onto the build platform for the scanning process. This process continues until the fabrication of the complete model finishes. The whole process is carried out in an inert atmosphere to avoid the oxidation, degradation, and interaction of the molten metal with the surroundings[1–4].

Here, each powder layer is a cumulative of multiplesingle scan tracks on the design data.Therefore, final partquality in SLM greatly depends on the quality of each single scan track and the interaction between each single scan track. Hence, single scan track analysis/observations become most significant for obtaining highly dense fabricated products. In SLM process, single scan track melt pool geometry and dimensions not only depend on various machine parameters such as laser power, scan speed, layer thickness, laser beam radius, type of laser source, inert gas flow, build platform temperature etc. andalso various material properties such as absorptivity, heat conductivity, specific heat, melting point, density etc. These are all very important analyses for the SLM process to fabricate highly dense products. Parts fabricated using SLM often encounter build defects during printing such as cracks, porosity, delamination of layers, balling, and keyhole etc. due to lack in understanding of the SLM process (molten metal fluid flow, material absorptivity, laser parameters, temperature distribution, material phase changes and microstructural changes etc.). Now a days it has become important to understand the SLM process to achieve the high dense and customized components with high build rates. In single scan track, the effect of linear energy density is related asequation 1

$$L.E = \frac{p}{v} \text{ J/mm---------- (1)}$$

Where L.E = linear energy density

p = laser power

v = scan speed

In SLMprocess, further the energy density requires for the fabrication is related as shown in equation 2.

$$E = \frac{P}{v*h*t} J/mm^3 \text{----------(2)}$$

Where, E = volumetric energy density, h = hatch spacing, t = powder bed layer thickness, v = scan speed and P = laser power

In SLM process, there are various types of defects (lack of fusion porosity, keyholing, balling, cracks etc.) present which create problem in achieving the high dense components. It is major challenge in SLM to understand and avoid these defects with varying different processing parameters to achieve the high-quality components[5–13].

In order to understand the complete SLM process, single scan strategy needs to be understood properly as explained above. Hence, attempt was made to understand single scan strategy by varying the laser power and scan speed. Based on the developed printed layer defects and melt pool analysis was carried out and the results are compared with the available literatures.

2. Experimental procedure:

AlSi10Mg gas atomized powder purchased from EOS, GmbH, Germany was used for the experiment. Powder was spherical in shape and composition is given in Table 1. Selective laser melting (EOS M 290) machine having fibre laser of 400 W laser powers was used for this experiment.

Table 1: Elemental composition of as-purchased AlSi10Mg powder used for SLM process

Element	Si	Mg	Fe	Mn	Cu	Zn	Ti	Al
Percentage	10	0.45	0.25	<0.005	<0.005	<0.002	<0.01	Balance

For the optimization of processparameters, total 5 different laser powers (200, 250, 300, 350, and 370 W) with 8 different scan speeds (300, 500, 700, 900, 1100, 1300, 1500, 1700 mm/s) were

selected. Line energy was calculated for all the conditions and mentioned in Table 2. For the total optimization process parameters, layer thickness (30 μm), and laser spot size (80 μm) were kept constant and the complete printing process was carried out in argon gas atmosphere to avoid the oxidation of powder. These single tracks were cut using EDM wire cut (CUT E600)and analysis was carried out using optical microscope (Lieca DM2700). Single scans were observed for the discontinuity and presence of defects if any. Cross section of single scan tracks were polished using series of SiC papers ranging from 400 to 2500 grades followed by disk cloth polishing using diamond pastes (6-12, 3-4, 0.5-1, 1, and 0.5 microns). Subsequently, the surface was etched using keller's reagent (2.5 vol% of HNO_3,1vol% HF, 1.5 vol% HCl, and 95 vol% distilled water) for 30 sec to reveal the melt pool cross section, and dimensions. These melt pool cross section was examined and dimensions were measured using optical microscope interactive measurement software. The graphical representation of the melt pool dimension is shown in Figure 1.

Table 2: Experimental processing parameters and line energy densities of AlSi10Mg

Laser power(W)	Scan speed (mm/s)	Line energy density(J/mm)
200	300	0.67
200	500	0.4
200	700	0.28
200	900	0.22
200	1100	0.18
200	1300	0.15
200	1500	0.13
200	1700	0.12
250	300	0.83
250	500	0.5
250	700	0.36
250	900	0.28
250	1100	0.23
250	1300	0.19
250	1500	0.17
250	1700	0.15
300	300	1
300	500	0.6
300	700	0.43
300	900	0.33
300	1100	0.27
300	1300	0.23
300	1500	0.2
300	1700	0.18
350	300	1.17
350	500	0.7
350	700	0.5
350	900	0.39
350	1100	0.32
350	1300	0.27
350	1500	0.23
350	1700	0.21
370	300	1.23
370	500	0.74
370	700	0.53
370	900	0.41
370	1100	0.34
370	1300	0.28
370	1500	0.25
370	1700	0.22

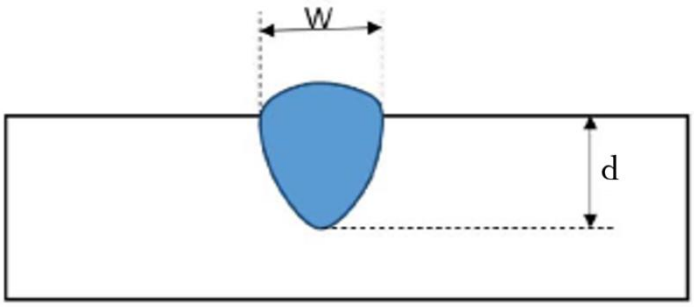

Fig 1: Schematic representation of melt pool analysis in the single scan track.

3. Results and discussions

3.1 UV-DRS analysis

Absorptivity is one of the important material properties which affect the SLM process. Based on the absorptivity, heat energy in the SLM process temperature in the melt pool can be determined. Absorptivity of AlSi10Mg powder was obtained from the UV-DRS method and the result is shown in Figure 2. The absorptivity of 0.45 was obtained from the analysis as fibre laser in the EOS M 290 wavelength was 1080 nm.

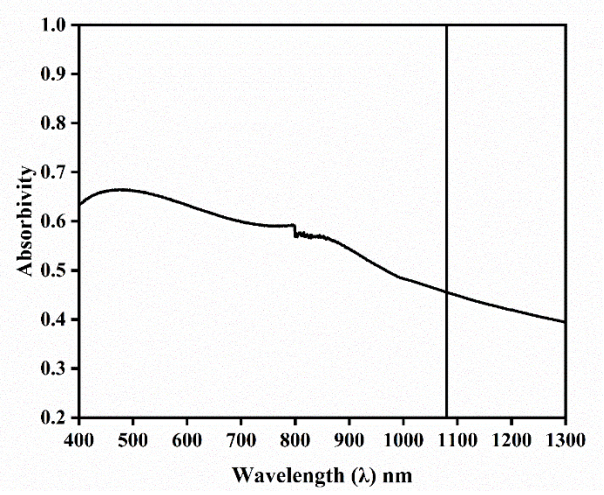

Fig 2: Absorptivity spectra of AlSi10Mg as measured from UV-DRS.

3.2 Melt pool analysis

Single scan track deposits were successfully made on the aluminium substrate using the listed laser parameters as shown in Table 2. By the single scan track analysis, it is possible to predict the defect formation in the manufacturing process and identify the better processing parameters. In SLM, lack of fusion and keyhole porosities are common defects those can be predicted by the single scan track analysis.

3.2.1 Lack of fusion porosity

Lack of fusion porosity will occur when melt pool does not cover full area in the powder bed layer in terms of width, depth, and hatch spacing distance creating an area of un-melted region. These un-melted particles will create the porosity and lowers the mechanical properties. According to studies, lack of fusion porosity depends on the energy density and however, later it was found that other important aspects such as hatch space, layer thickness and melt pool dimensions are also responsible for such defects formation as shown in the equation 3.

$$\left(\frac{H}{w}\right)^2 + \left(\frac{L}{d}\right)^2 \leq 1 \quad \text{---------- 3}$$

Where, H – hatch spacing, w – melt pool width, L – layer thickness and d – melt pool depth

3.2.2 Keyhole porosity

When the energy density is sufficient, metal will vaporize in the powder layer and create the pressure. The force generated during vaporization will create the vapour cavity in the melt pool and pushes the melt pool to the deeper which creates narrow and deeper melt pool. This phenomenon is called as keyhole-mode. Sometimes the developed vapour cavity closes before the escape of gas and creates the gas porosity in the melt pool. The keyholing phenomenon

depends on lot of parameters like absorptivity, enthalpy of melting, melting point, density, laser related parameters like power, speed, and size of laser beam etc. The normalized enthalpy is determined from the energy distributed in a unit volume ΔH, divided by the enthalpy of melting h_s as shown in equation 4 and 5.

$$\frac{\Delta H}{h_s} = \frac{AP}{\pi h_s \sqrt{vD\sigma^3}}; h_s = \rho c_p t_m \text{ ----------4}$$

$$\frac{\Delta H}{h_s} > \frac{\pi t_b}{t_m} \text{ ---------- 5}$$

Where A – powder absorptivity, p – laser power, v – laser scanning speed

D – thermal diffusivity, σ – laser spot size, ρ – density, c_p – specific heat

If equation 5 satisfied then mode of melting is considered as keyhole mode. Porosity from the keyhole is observed as spherical and it differs from lack of fusion porosity [7-12, 14-30].

Single scan tracks were observed using optical microscope to analyse the discontinuity and defects present in the scan track and the result is shown in Figure 3. From Figure 3 it was observed that as laser power increases from 200 to 370 W, scan track thickness increases. Further, if scan speed increases from 300 to 1700 mm/s the scan track thicknessagain decreases. However, all scan tracks were continuous and no discontinuous tracks were present for the listed processing parameters considered in the present study.

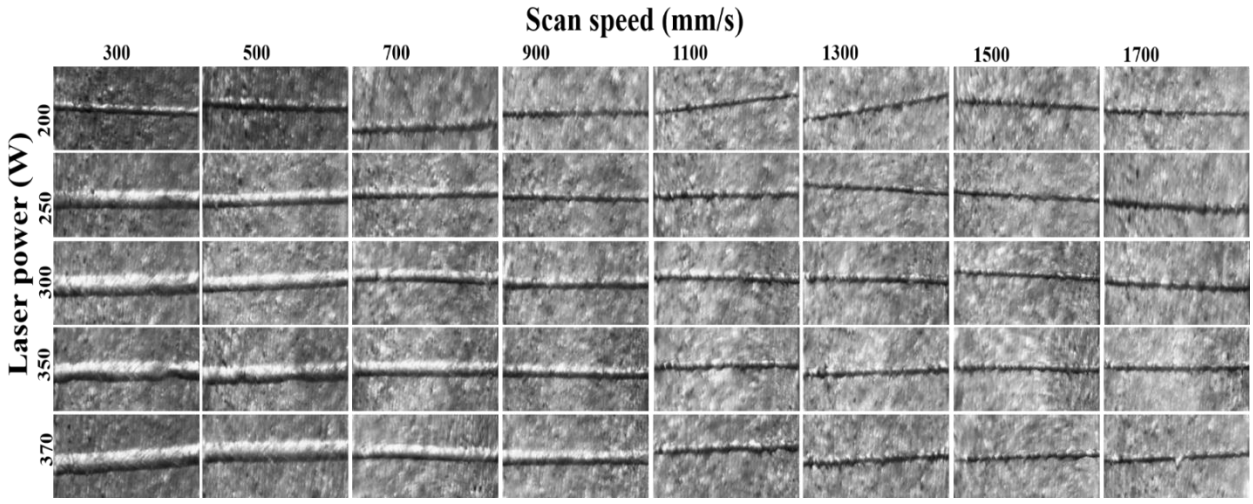

Fig 3: Single scan tracks of AlSi10Mg deposited on the aluminium substrate.

Cross-section of single scan tracks were examined for the melt pool dimensions and defects present in the melt pool such as cracks and pores. No cracks and pores were found in the single scan tracks cross-section analysisas shown in Figure 4. These melt pool analyses also helps to increase the build rate of the manufacturing process by optimizing the process parameters as shown in equation 6.

Building rate (mm^3/s) = v * H * L ---------- 6

Building rate directly proportional to the scan speed, hatch spacing, and layer thickness and here by optimizing these parameters it is possible to achieve high build rate with high density products. Dimensions of melt pool will be useful in determining the optimum hatch spacing and layer thickness required for the manufacturing without compromising the density of alloy using the equations 3 and 4.

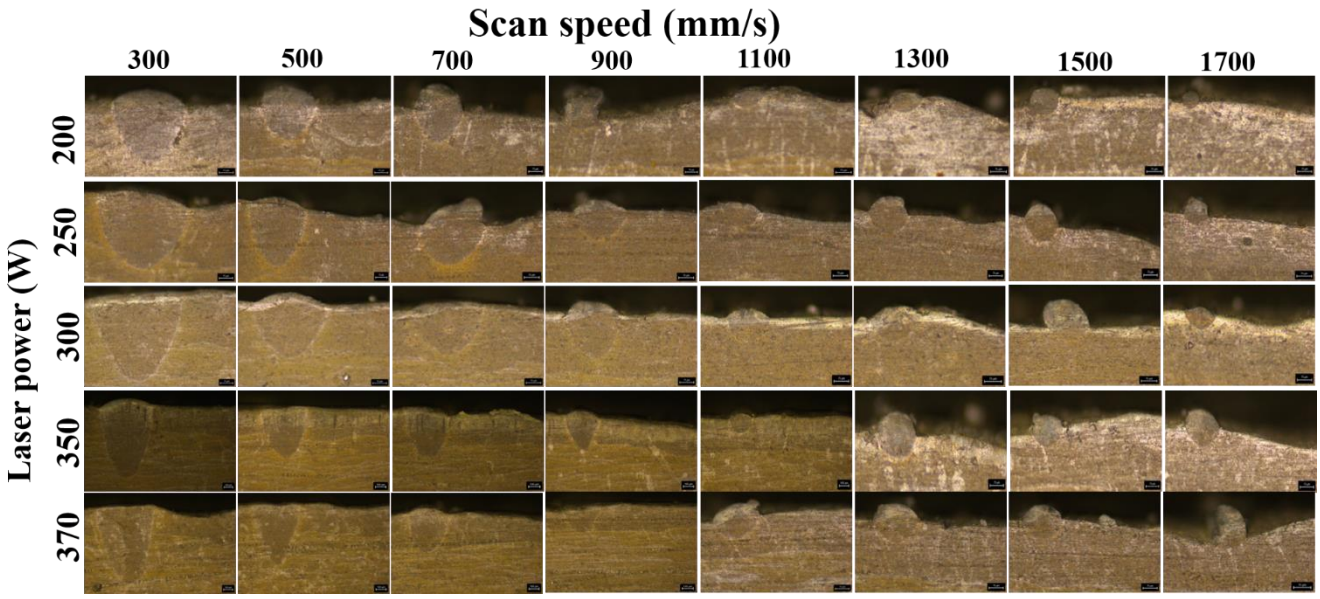

Fig 4: Cross-sectional image of AlSi10Mg single scan tracks.

From the Figure 5 of melt pool depth analysis,it was evident that as laser power increases the depth of the melt pool increases. This increased laser power generates more heat and thisheat will penetrate deeperthereby increasing thedepth of melt pool.

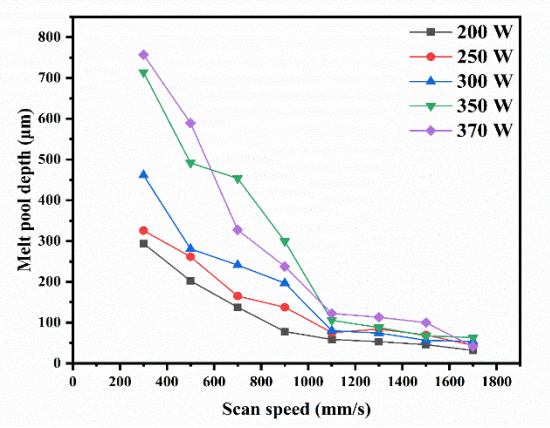

Fig 5: Depth profile of AlSi10Mg single scan tracks

On the other hand, as laser scan speed increases depth of melt pool reduces because exposure time of laser will decrease and hence, it will decrease the heat generation in the powder

bed and causes the decrease in depth of melt pool. Width of the melt pool also follows the same trend as melt pool depth as shown in Figure 6.

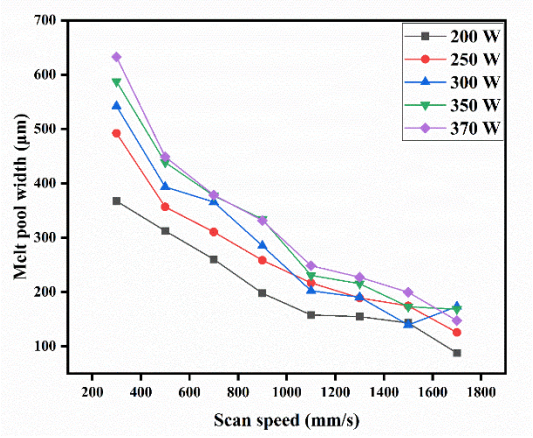

Fig 6: Width profile of AlSi10Mg single scan tracks.

Further, with the increase in laser power from 200 to 370 W, melt pool width showed an increasein trend. This is mainly attributed to the increased heat generated in the powder bed which increase the width of the melt pool. As laser scan speed increases, width of the melt pool decreases. Because heat generated in the powder bed decreases with increase in scan speed due to this width of the melt pool again decreases.

4 Conclusions:

AlSi10Mg single scan track deposits were successfully made on the aluminium substrate using the given laser parameters (power and scanning speed). From the deposited scan tracks it was observed that there are no discontinuous tracks were deposited by given parameters. From the cross-section of scan tracks it was observed that there are no cracks and pores were present in the melt pool. From the dimensions of melt pool analysis, it was found that as laser power increases from 200 to 370 W depth and width of the melt pool increases and as laser scan speed increases from 300 to 1700 mm/s width of the melt pool showed a decreasing trend. By optimizing the

melt pool dimensions, hatch spacing and layer thickness can be determined and it will be useful in increasing the build rate without compromising the quality of final product.

Acknowledgements:

BSC and MS are grateful for the fellowship from CSIR-SRF (31/GATE/20(33)/2020- EMR-I) and (31/GATE/20(32)/2020-EMR-I) respectively. All the authors are thankful to the Additive manufacturing facility staff for sample preparation and Central instrumentation facility staff for the characterization.

References:

[1] A. Mauduit, S. Pillot, and H. Gransac, "Study of the suitability of aluminum alloys for additive manufacturing by laser powder-bed fusion," *UPB Sci. Bull. Ser. B Chem. Mater. Sci.*, vol. 79, no. 4, pp. 219–238, 2017.

[2] T. Fiedler, K. Dörries, and J. Rösler, "Selective laser melting of Al and AlSi10Mg: parameter study and creep experiments," *Prog. Addit. Manuf.*, vol. 7, no. 4, pp. 583–592, 2022, doi: 10.1007/s40964-021-00248-5.

[3] H. Hyer *et al.*, "Understanding the Laser Powder Bed Fusion of AlSi10Mg Alloy," *Metallogr. Microstruct. Anal.*, vol. 9, no. 4, pp. 484–502, 2020, doi: 10.1007/s13632-020-00659-w.

[4] Z. Wang *et al.*, "Selective laser melting of aluminum and its alloys," *Materials (Basel).*, vol. 13, no. 20, pp. 1–67, 2020, doi: 10.3390/ma13204564.

[5] Y. Li and D. Gu, "Parametric analysis of thermal behavior during selective laser melting additive manufacturing of aluminum alloy powder," *Mater. Des.*, vol. 63, pp. 856–867,

2014, doi: 10.1016/j.matdes.2014.07.006.

[6] S. Shrestha and K. Chou, “Single track scanning experiment in laser powder bed fusion process,” *Procedia Manuf.*, vol. 26, pp. 857–864, 2018, doi: 10.1016/j.promfg.2018.07.110.

[7] Y. Yang *et al.*, “Validated dimensionless scaling law for melt pool width in laser powder bed fusion,” *J. Mater. Process. Technol.*, vol. 299, 2022, doi: 10.1016/j.jmatprotec.2021.117316.

[8] X. Ao, H. Xia, J. Liu, and Q. He, “Simulations of microstructure coupling with moving molten pool by selective laser melting using a cellular automaton,” *Mater. Des.*, vol. 185, no. October, p. 108230, 2020, doi: 10.1016/j.matdes.2019.108230.

[9] B. Cheng, X. Li, C. Tuffile, A. Ilin, H. Willeck, and U. Hartel, “Multi-physics modeling of single track scanning in selective laser melting: Powder compaction effect,” *Solid Free. Fabr. 2018 Proc. 29th Annu. Int. Solid Free. Fabr. Symp. - An Addit. Manuf. Conf. SFF 2018*, no. January 2019, pp. 1887–1902, 2020.

[10] N. Chen *et al.*, “Effect of ambient pressure on laser welding of AlSi10Mg fabricated by selected laser melting,” *Mater. Des.*, vol. 215, p. 110427, 2022, doi: 10.1016/j.matdes.2022.110427.

[11] M. Letenneur, A. Kreitcberg, and V. Brailovski, “Optimization of laser powder bed fusion processing using a combination of melt pool modeling and design of experiment approaches: Density control,” *J. Manuf. Mater. Process.*, vol. 3, no. 1, 2019, doi: 10.3390/jmmp3010021.

[12] D. Martínez-Maradiaga, O. V. Mishin, and K. Engelbrecht, “Thermal Properties of Selectively Laser-Melted AlSi10Mg Products with Different Densities,” *J. Mater. Eng. Perform.*, vol. 29, no. 11, pp. 7125–7130, 2020, doi: 10.1007/s11665-020-05192-z.

[13] I. Yadroitsev, A. Gusarov, I. Yadroitsava, and I. Smurov, “Single track formation in selective laser melting of metal powders,” *J. Mater. Process. Technol.*, vol. 210, no. 12, pp. 1624–1631, 2010, doi: 10.1016/j.jmatprotec.2010.05.010.

[14] M. S. Kim, “Effects of processing parameters of selective laser melting process on thermal conductivity of alsi10mg alloy,” *Materials (Basel).*, vol. 14, no. 9, 2021, doi: 10.3390/ma14092410.

[15] L. Cai and S. Y. Liang, “Analytical modelling of temperature distribution in slm process with consideration of scan strategy difference between layers,” *Materials (Basel).*, vol. 14, no. 8, 2021, doi: 10.3390/ma14081869.

[16] P. Promoppatum and S. C. Yao, “Analytical evaluation of defect generation for selective laser melting of metals,” *Int. J. Adv. Manuf. Technol.*, vol. 103, no. 1–4, pp. 1185–1198, 2019, doi: 10.1007/s00170-019-03500-z.

[17] W. E. King *et al.*, “Observation of keyhole-mode laser melting in laser powder-bed fusion additive manufacturing,” *J. Mater. Process. Technol.*, vol. 214, no. 12, pp. 2915–2925, 2014, doi: 10.1016/j.jmatprotec.2014.06.005.

[18] S. Patel, H. Chen, M. Vlasea, and Y. Zou, “The influence of beam focus during laser powder bed fusion of a high reflectivity aluminium alloy — AlSi10Mg,” *Addit. Manuf.*, vol. 59, 2022, doi: 10.1016/j.addma.2022.103112.

[19] C. Schwerz and L. Nyborg, “Linking in situ melt pool monitoring to melt pool size distributions and internal flaws in laser powder bed fusion,” *Metals (Basel).*, vol. 11, no. 11, 2021, doi: 10.3390/met11111856.

[20] M. Khorasani *et al.*, “A comprehensive study on meltpool depth in laser-based powder bed fusion of Inconel 718,” *Int. J. Adv. Manuf. Technol.*, vol. 120, no. 3–4, pp. 2345–2362, 2022, doi: 10.1007/s00170-021-08618-7.

[21] W. Wang, J. Ning, and S. Y. Liang, “Analytical prediction of keyhole porosity in laser powder bed fusion,” *Int. J. Adv. Manuf. Technol.*, vol. 119, no. 11–12, pp. 6995–7002, 2022, doi: 10.1007/s00170-021-08276-9.

[22] J. Kim, S. Lee, J. K. Hong, N. Kang, and Y. S. Choi, “Calibration of Laser Penetration Depth and Absorptivity in Finite Element Method Based Modeling of Powder Bed Fusion Melt Pools,” *Met. Mater. Int.*, vol. 26, no. 6, pp. 891–902, 2020, doi: 10.1007/s12540-019-00599-3.

[23] M. Tang, P. C. Pistorius, and J. L. Beuth, “Prediction of lack-of-fusion porosity for powder bed fusion,” *Addit. Manuf.*, vol. 14, pp. 39–48, 2017, doi: 10.1016/j.addma.2016.12.001.

[24] B. Cheng, L. Loeber, H. Willeck, U. Hartel, and C. Tuffile, “Computational Investigation of Melt Pool Process Dynamics and Pore Formation in Laser Powder Bed Fusion,” *J. Mater. Eng. Perform.*, vol. 28, no. 11, pp. 6565–6578, 2019, doi: 10.1007/s11665-019-04435-y.

[25] S. P. Narra, L. Scime, and J. Beuth, “Integrated Control of Melt Pool Geometry and

Microstructure in Laser Powder Bed Fusion of AlSi10Mg," *Metall. Mater. Trans. A Phys. Metall. Mater. Sci.*, vol. 49, no. 10, pp. 5097–5106, 2018, doi: 10.1007/s11661-018-4804-z.

[26] J. Ning, W. Wang, X. Ning, D. E. Sievers, H. Garmestani, and S. Y. Liang, "Analytical thermal modeling of powder bed metal additive manufacturing considering powder size variation and packing," *Materials (Basel).*, vol. 13, no. 8, 2020, doi: 10.3390/MA13081988.

[27] T. Wang, Y. Wang, C. Chen, and H. Zhu, "Relationships between the characteristics of porosity, melt pool and process parameters in laser powder bed fusion Al Zn alloy," *J. Manuf. Process.*, vol. 68, no. PA, pp. 1236–1244, 2021, doi: 10.1016/j.jmapro.2021.06.027.

[28] H. Wang and Y. Zou, "Microscale interaction between laser and metal powder in powder-bed additive manufacturing: Conduction mode versus keyhole mode," *Int. J. Heat Mass Transf.*, vol. 142, no. August, 2019, doi: 10.1016/j.ijheatmasstransfer.2019.118473.

[29] H. Ghasemi-Tabasi, J. Jhabvala, E. Boillat, T. Ivas, R. Drissi-Daoudi, and R. E. Logé, "An effective rule for translating optimal selective laser melting processing parameters from one material to another," *Addit. Manuf.*, vol. 36, no. April, p. 101496, 2020, doi: 10.1016/j.addma.2020.101496.

[30] B. Zhang, Y. Li, and Q. Bai, "Defect Formation Mechanisms in Selective Laser Melting: A Review," *Chinese J. Mech. Eng. (English Ed.*, vol. 30, no. 3, pp. 515–527, 2017, doi: 10.1007/s10033-017-0121-5.